

MapleGrasp: Mask-guided Feature Pooling for Language-driven Efficient Robotic Grasping

Vineet Bhat

Naman Patel

Prashanth Krishnamurthy

Ramesh Karri

Farshad Khorrami

New York University Tandon School of Engineering
Brooklyn, NY, USA

vrb9107@nyu.edu

Abstract

Robotic manipulation of unseen objects via natural language commands remains challenging. Language driven robotic grasping (LDRG) predicts stable grasp poses from natural language queries and RGB-D images. We propose MapleGrasp, a novel framework that leverages mask-guided feature pooling for efficient vision-language driven grasping. Our two-stage training first predicts segmentation masks from CLIP-based vision-language features. The second stage pools features within these masks to generate pixel-level grasp predictions, improving efficiency, and reducing computation. Incorporating mask pooling results in a 7% improvement over prior approaches on the OCID-VLG benchmark. Furthermore, we introduce RefGraspNet, an open-source dataset eight times larger than existing alternatives, significantly enhancing model generalization for open-vocabulary grasping. MapleGrasp scores a strong grasping accuracy of 89% when compared with competing methods in the RefGraspNet benchmark. Our method achieves comparable performance to larger Vision-Language-Action models on the LIBERO benchmark, and shows significantly better generalization to unseen tasks. Real-world experiments on a Franka arm demonstrate 73% success rate with unseen objects, surpassing competitive baselines by 11%. Code is available here: <https://github.com/vineet2104/MapleGrasp>

1. Introduction

The ability to perceive and interact with objects in an environment is a defining characteristic of human intelligence. As humans mature, we develop capabilities to manipulate novel objects, generalizing our understanding beyond previous experiences. Replicating this intelligence in robotics remains a formidable challenge. Robots often encounter unfamiliar objects and must adapt to new scenarios without

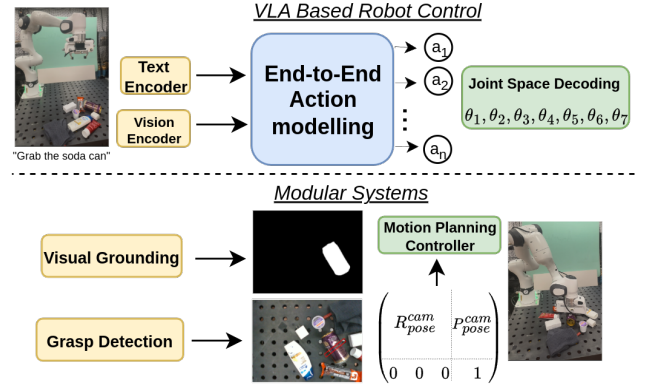


Figure 1. Modular systems generate object masks and grasp poses, utilizing a control algorithm to estimate joint space trajectories, while VLAs directly map vision and textual modalities to actions.

prior knowledge [27]. Foundational models, particularly Vision-Language Models (VLMs), aim to bridge this gap by leveraging extensive pre-trained multi-modal representations to enhance robotic perception and interaction [23, 62].

An autonomous robotic manipulation framework typically comprises four key stages: task planning, visual grounding, object manipulation, and goal-oriented placement. Recent advances have demonstrated the effectiveness of VLMs across these stages, incorporating large-scale pre-trained representations to improve generalization [51]. An alternative paradigm involves Vision-Language-Action (VLA) models, which directly predict trajectories for grasping and manipulating objects, bypassing the modular pipeline [3, 11]. We highlight the difference in these two frameworks in Fig. 1. While VLAs have shown remarkable performance in tasks across both simulation and real-world settings, their deployment in novel environments presents three key challenges: **i) Task-Specific Data Collection:** Collecting teleoperated or human demonstrations is often difficult and time-consuming for novel interactions [50]; **ii)**

Expensive fine-tuning: Large VLAs require task-specific fine-tuning, which is computationally expensive requiring hundreds of GPU hours. Although parameter-efficient fine-tuning (PEFT) techniques alleviate some costs, they restrict adaptability by modifying only a small subset of parameters [18]; **iii) Limited generalization:** Fine-tuned VLAs often fail to generalize in dynamic environments, particularly when objects are repositioned or when visually similar distractor objects are introduced [44]. Given these challenges, modular frameworks offer an attractive alternative that balances generalizability with ease of deployment. By decoupling perception, planning, and manipulation, modular architectures allow state-of-the-art models in each component to be independently improved and integrated as research advances. Furthermore, LLM-agentic frameworks can serve as high-level decision-makers, dynamically invoked perception and manipulation modules for task execution in novel environments [13, 36, 38]. Compounded errors within modular frameworks can be mitigated using closed-loop feedback and error planning [5, 14].

In this work, we focus on a critical capability within modular frameworks, language-driven grasp detection. This task predicts a stable grasp pose for a specified object based on RGB-D images and a free-form language expression. An accurate LDRG model can enable low-level execution for high-level LLM planners, advancing fully autonomous agentic frameworks for human-robot interaction. Our proposed method, MapleGrasp, can predict both 4 DoF top-down and oriented 6 DoF grasps. Our contributions include:

1. A novel two-stage training architecture for LDRG: initial text-referred object mask prediction, followed by mask-guided feature pooling for grasp refinement.
2. Empirical evidence that restricting grasp predictions to mask-pooled regions leads to faster and more efficient training, while achieving better accuracy against previous methods by 7% on the OCID-VLG benchmark.
3. Introduce RefGraspNet, a large-scale open-source benchmark comprising over 200 million grasps, eight times larger than existing datasets (Tab. 1), consisting of challenging real-world scenarios for grasping.
4. Extensive comparisons with VLAs in a physics simulated environment demonstrate strong performance and improved generalization to novel tasks. MapleGrasp robustly transfers to real-world trials with the Franka arm, achieving 87% and 73% grasping success rates in seen and unseen environments, respectively, surpassing previous methods by more than 11%.

2. Related Works

Grasp Detection. Robotic grasping with parallel grippers has been extensively studied in both the 2D and 3D domains. The 4-DoF grasp representation defines a grasp using four parameters: (x, y) as the center of the grasp, w

as the grasp width, and θ as the grasp axis angle relative to a top-down hand orientation [1, 7, 15]. The 6-DoF representation extends this to 3D, incorporating three degrees of translation and three degrees of rotation required for stable object grasping [9, 29, 39]. The use of RGB-D data has shown promising results for precision grasping, where CNN and ResNet-based architectures leverage visual features to predict grasp pose parameters [20, 46, 56, 63]. Recent advancements in transformer architectures and self-supervised learning have bridged the gap between vision and textual modalities, shifting research towards incorporating language as an additional modality for object manipulation [51]. Language-driven grasp detection (LDGD) refers to the task of associating referring text expressions with RGB-D images to predict a suitable robotic grasp pose for object manipulation [47]. Two primary approaches have emerged for LDGD: i) Visual grounding of referring expressions: Predicts segmentation masks for the target object [6, 53, 60], followed by pre-trained grasp detection networks to compute grasp poses [2, 25, 30]. ii) End-to-end grasp pose estimation: Directly predicts grasp poses from input text and RGB-D images [49, 54, 61].

End-to-End Language-Driven Grasping. Recent work has introduced diffusion models that learn a probabilistic diffusion process to generate grasp poses during inference [32, 33, 47]. Vision-language fusion provides an alternative approach, offering faster convergence and lower inference times [22, 31, 51]. The ETRG framework enhances vision-language feature fusion for grasp detection by integrating trainable adapters into frozen CLIP vision and text encoders [55]. MaskGrasp employs a tri-head architecture with cross-attention mechanisms using text embeddings, region-of-interest feature embeddings, and mask embeddings [45]. GraspSAM adapts the Segment Anything Model [19] for grasp detection and utilizes GroundingDINO [26] to transform text expressions into object bounding boxes [34]. GraspMolmo [8] trains the Molmo VLM on the grasp point detection task followed by a grasp proposal sampler to identify accurate grasps for task oriented grasping. Our proposed architecture predicts grasp pose using quality, width and angle maps. Several studies have explored similar setups for LDGD [41, 43, 44]. These maps can be used to predict both 4 DoF and 6 DoF grasps by computing the grasp point on the object and overlapping with an independent grasp proposal network.

In this work, we study mask pooling for grasp detection and demonstrate that localizing the grasp prior to predicting its angle and width leads to a more efficient learning process. This approach improves both training efficiency and test-time accuracy. Additionally, we present the first comprehensive comparison of LDRG approaches with large VLAs in the context of language-guided grasping tasks.

Vision-Language-Action Models. Direct modeling of vi-

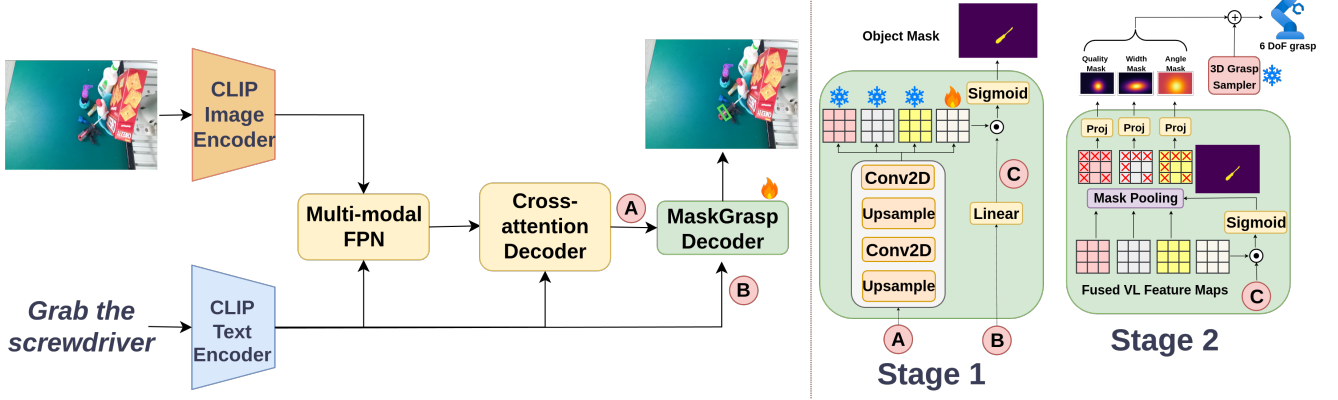


Figure 2. MapleGrasp: Our framework trains on fused vision-language embeddings for object segmentation, then applies mask pooling in grasp prediction heads. The predicted grasp maps can be used for both top-down and oriented grasping.

sion and language modalities for joint-space robotic control has gained significant interest in recent research. Advances in vision-language models [16, 28, 58], coupled with the availability of large-scale robotic datasets spanning diverse environments, hardware platforms, and tasks [4], have enabled the training of Vision-Language-Action (VLA) models for robotic manipulation [12, 24, 35]. However, the large model sizes of VLAs often demand substantial GPU resources for fine-tuning and real-world deployment [48]. Recent research has sought to mitigate these computational challenges through parameter-efficient training techniques and action chunking [17, 18], enabling deployment on smaller GPUs with real-time kernel compatibility.

3. Methodology

We propose object-mask feature pooling to isolate relevant regions for grasp detection in clutter, detail our architecture (Fig. 2), and outline an enhanced training objective.

3.1. Language-Driven Grasp Detection

From an RGB-D image and a referring expression identifying a target object to grasp, language-driven grasping models must predict a stable grasp pose for a parallel gripper or dexterous hand. This poses three primary challenges: (i) identifying the target from textual cues (color, shape, spatial relations); (ii) selecting a collision-free grasp executable in real settings; and (iii) generalizing to unseen objects. Vision-language driven grasping is studied with both 4 DoF top-down and 6 DoF oriented grasps. While 6 DoF grasps are more accurate, annotating such grasp poses at a large scale to create real-world datasets is challenging. A number of works thus rely on image-based datasets with 4 DoF grasp rectangles. We design our method such that it can be used with both 4 DoF and 6 DoF grasping datasets. Fig. 3 illustrates the two grasp formats and their transformation via an external proposal sampler.

Formally, MapleGrasp predicts three dense maps, each of size $H \times W$: a grasp quality map $Q \in \mathbb{R}^{H \times W}$, a grasp

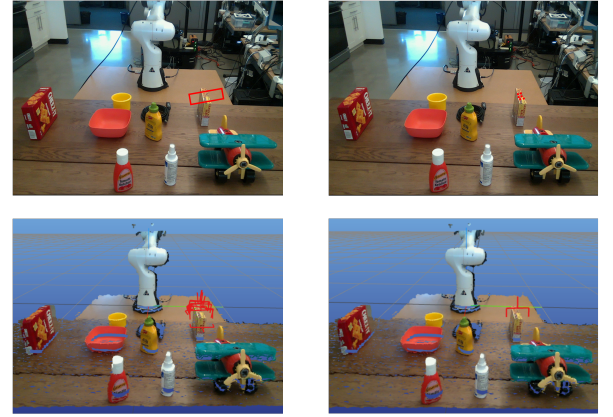


Figure 3. Conversion from a 4 DoF to a 6 DoF grasp pose: (top-left) initial top-down grasp rectangle, (top-right) sampled contact points reprojected to 2D, (bottom-left) 6 DoF grasp proposals from Contact-GraspNet [40], (bottom-right) selected 6 DoF grasp.

width map $w \in \mathbb{R}^{H \times W}$, and a grasp angle map $\theta \in \mathbb{R}^{H \times W}$. The quality map assigns a score to each pixel, indicating the likelihood of a successful grasp. The width map encodes the optimal gripper width at each pixel, while the angle map represents the in-plane grasp orientation $\theta \in [-\pi/2, \pi/2]$. A 2D rectangular grasp $g_{2D} = (x^*, y^*, w^*, \theta^*)$ is extracted by selecting the pixel $(x^*, y^*) = \arg \max_{(i,j)} Q_{i,j}$, and reading $w^* = w_{x^*, y^*}$, $\theta^* = \theta_{x^*, y^*}$. This rectangular grasp is projected onto the point cloud \mathcal{P} to identify a subset of points $\mathcal{P}_g \subset \mathcal{P}$ within the grasp rectangle. A set of candidate 6-DoF grasp poses $\{G_k\}$ is generated using an independent grasp sampler. Each candidate pose G_k is evaluated by computing its intersection with \mathcal{P}_g , and the final grasp G^* is chosen as the one that overlaps the maximum number of graspable points: $G^* = \arg \max_k |\mathcal{P}_g \cap \mathcal{V}(G_k)|$, where $\mathcal{V}(G_k)$ denotes volume swept by the gripper pose G_k .

3.2. Motivation for Mask Pooling

Most LDRG methods predict an object mask and grasp pose simultaneously. A binary object segmentation mask already pinpoints the pixels referenced by the query, implicitly limiting where a valid grasp can lie. If the mask is correct, the grasp network need not evaluate locations outside it, shrinking search space and reducing errors. We treat the mask as an explicit *guiding mechanism*: features are pooled within the segmented region before grasp prediction.

3.3. MapleGrasp

Given an RGB image $I \in \mathbb{R}^{H \times W \times 3}$ and a referring instruction T , we compute vision-language embeddings using a pre-trained CLIP model: $x_{\text{img}} = \text{CLIP}_{\text{img}}(I)$, $x_{\text{text}} = \text{CLIP}_{\text{text}}(T)$. The visual embedding x_{img} is passed through a multi-modal Feature Pyramid Network \mathcal{F} , and fused with the text embedding via cross-attention, resulting in $x_{\text{fused}} = \text{CrossAttn}(\mathcal{F}(x_{\text{img}}, x_{\text{text}}), x_{\text{text}})$. These embeddings are then processed through a series of convolutional and upsampling layers to produce a spatial feature map $f \in \mathbb{R}^{H' \times W' \times C}$, where H' and W' are intermediate spatial resolutions and C is the channel dimension. We introduce *Mask-Guided Feature Pooling* within a two-stage training framework to guide grasp prediction. In **Stage I (Segmentation Training)**, we freeze the grasp prediction heads and train the segmentation branch independently. The text embedding x_{text} is projected via a linear layer to obtain $z \in \mathbb{R}^C$, which is then used to compute the object-centric mask via a per-pixel dot product: $M_{i,j} = \sigma(f_{i,j}^\top z)$, yielding a soft binary mask $M \in [0, 1]^{H' \times W'}$. This stage allows mild overfitting to ensure accurate object localization for downstream pooling. In **Stage II (Mask-Guided Grasp Prediction)**, we train the full model end-to-end. The predicted mask M is used to modulate the visual features via element-wise multiplication, producing $f_{\text{pooled}} = f \odot M$. These pooled features are refined and passed through three parallel projection heads to predict the grasp quality $Q = \mathcal{H}_q(f_{\text{pooled}})$, angle $\theta = \mathcal{H}_\theta(f_{\text{pooled}})$, and width $w = \mathcal{H}_w(f_{\text{pooled}})$.

Our goal was to support both 4-DoF and 6-DoF grasping with minimal architectural changes for future dataset compatibility. For image-only datasets with 4-DoF grasp pose annotations, we utilize the grasp rectangle to compute ground truth quality, angle, and width maps, following prior work [44]. For RGB-D datasets with 6-DoF grasp poses, we first identify the 3D area on the target object where ground truth poses occur. This region is then projected into 2D to generate a rectangle over the graspable area of the object, which is subsequently treated in a manner analogous to the 4-DoF case. MapleGrasp computes the graspable region on the object, which is then overlapped with candidate 6-DoF grasp poses generated by an off-the-shelf grasp sampler, Contact-GraspNet [40]. The candidate with maximum overlap is selected as the collision-free grasp for the target.

3.4. Loss Function

Prior work utilizes the Smooth L1 loss for pixel-wise prediction in visual grounding, defined per pixel (\hat{x}_p, x_p) as:

$$L_{\text{smoothL1}}(\hat{x}_p, x_p) = \begin{cases} \frac{(\hat{x}_p - x_p)^2}{2\beta}, & \text{if } |\hat{x}_p - x_p| < \beta, \\ |\hat{x}_p - x_p| - \frac{\beta}{2}, & \text{otherwise.} \end{cases} \quad (1)$$

Here, $\hat{x}_p \in \mathbb{R}$ denotes predicted value at pixel p , $x_p \in \mathbb{R}$ is the ground-truth value, and $\beta > 0$ is a constant that determines the transition point between L2 and L1 loss regions.

We extend this to formulate weighted Smooth L1 loss $w_p L_{\text{smoothL1}}(\hat{x}_p, x_p)$, by assigning per-pixel weights $w_p = 1 + \alpha Q_{\text{gt},p}$, where $Q_{\text{gt},p} \in [0, 1]$ is the ground-truth *quality map* indicating the object grasp region. By emphasizing suitable grasp regions, we enhance precise grasp estimation. Our experiments demonstrate that this modified loss function is beneficial in low-resource settings, where the dataset contains only single grasp annotation per object, ensuring more reliable and efficient learning.

3.5. Metrics

Language-driven grasp poses are evaluated based on their correctness, feasibility, and overall quality, given a language instruction and the corresponding scene image. Quantitative evaluation is performed using grasp success rate for both Top-1 and Top-K predictions. For 4-DoF grasping, a prediction is considered successful if its rotation angle differs from the ground-truth by less than 30° , and its intersection-over-union (IoU) with the ground-truth grasp rectangle exceeds 0.25 [31, 45]. For 6-DoF grasping, success is determined if the selected grasp proposal corresponds to the ground-truth grasp for the referred object [8].

4. RefGraspNet Dataset: Learning to Grasp from 200M+ Grasp Poses

To advance language-driven robotic grasping, we introduce RefGraspNet, a richly annotated dataset of over **219 million** high-quality 6 DoF grasp poses, derived from real-world cluttered scenes. Building on GraspNet-1B [10], which provides over one billion sampled grasps with force-closure scoring comprising 88 distinct household and industrial objects arranged in hundreds of densely cluttered table-top scenarios. Each scene captured from multiple calibrated viewpoints yielded object masks and 6 DoF grasp poses.

We automate generating referring expressions using DeepSeek-VL [28], an open-source VLM. Starting from ten instruction templates (e.g., “Grasp the {object},” “Locate the {object}”), we expanded object mentions with color, shape, and spatial qualifiers in multi-object layouts (e.g., “Grasp the red cup behind the yellow bowl”). This yielded over 12.25M unique referring phrases, ensuring robust grounding of grasp commands in cluttered environ-

Dataset	Real/Simulated	No. of Images	Ref. Text	Unique Obj.	Grasp Poses	Obj. Masks	Avg. Obj./Img.
Jacquard [7]	✓	54K	✗	–	967K	✗	1
VMRD [59]	✓	4.5K	✗	31	51.5K	✗	3.5
OV-Grasp [21]	Both	–	63K	117	✗	✓	–
ACRONYM [9]	✗	–	✗	262	17.7M	✗	–
RoboRefIt [30]	✓	10.7K	50.7K	66	✗	✓	7.1
OCID-VLG [44]	✓	1.7K	89.6K	31	521K	✓	17.08
GraspAnything++ [47]	✗	994K	10M	236	33M	✗	3.4
Ours: RefGraspNet	✓	97K	12.25M	88	219M	✓	9.57

Table 1. Comparison of existing LDRG datasets. RefGraspNet provides 200M+ high quality grasps, object masks for each scene, and thus can be used to finetune both referring segmentation and grasping models.

ments. Grasp candidates were filtered using a 70% force-closure confidence threshold, which was selected based on extensive manual validation, resulting in 219 million validated 6 DoF grasps—roughly eight times larger than the previous largest language-driven grasp dataset. We provide comprehensive comparisons in Tab. 1, demonstrating improvements in scale, scene complexity, and linguistic variety. To support empirical studies, we split our objects into 70% “seen” (62 objects) and 30% “unseen” (26 objects), and generate train/val, test-seen, and test-unseen splits. This design enables evaluation of generalization to novel objects and arrangements. Examples are shown in Fig. 4.



Figure 4. Samples from RefGraspNet showcasing cluttered scenes with multiple viewpoints, with diverse objects, distractors, and grasping instructions. Only top-down grasps shown for brevity.

5. Experiments

We evaluate MapleGrasp on OCID-VLG and RefGraspNet, while comparing it to prior LDRG and VLA methods in both simulation and real-world settings.

5.1. Benchmark Comparisons

The OCID-VLG corpus [44] contains 1763 highly cluttered indoor tabletop RGB-D scenes with 31 unique objects. Objects have annotated 4-DoF grasp poses and segmentation masks, associated with referring expressions describing attributes such as color, shape, and relative position. With

89K unique (RGB-Text-Mask) tuples, it is the largest publicly available dataset for LDRG¹. We also provide a benchmark on our new contributed RefGraspNet corpus.

We evaluate various CLIP-based architectures on both datasets: CROG [44] utilizes CLIP embeddings with cross-attention, followed by MLP layers, to simultaneously predict object masks and grasp maps. HiFi-CS [2] employs a frozen CLIP model with FiLM-based fusion and upsampling to generate object masks, followed by grasp estimation using a separate frozen network. ETRG [55] introduces trainable adapters within the CLIP model to adapt it for grasping, and is trained on additional data to segment referring expressions and predict referring affordance. All baselines are trained for 50 epochs to ensure a fair comparison (see Tab. 2). We also include a strong zero-shot baseline that combines Molmo [6] for identifying the referred object, SAM 2 [37] for generating the object mask, and GraspNet [10] for predicting both 4-DoF and 6-DoF grasp poses. MapleGrasp achieves a 7% relative improvement in Top-1 success rate over previous state-of-the-art methods, demonstrating higher precision in grasp prediction in OCID-VLG. In RefGraspNet, MapleGrasp outperforms baselines for both seen and unseen objects, with a larger performance margin observed in the unseen setting. We attribute this to our closely coupled dual-stage training, which is able to provide partial object masks in unseen objects, which is then used by the grasp detection module to generate graspable object regions and accurate grasp poses. MapleGrasp trains more efficiently, converging in 32 epochs (~8 hours), compared to 45–50 epochs (12–16 hours) required by other baselines on an RTX 4090 GPU.

5.2. Qualitative and ablation studies

We provide comparisons in (Tab. 3). In row 1 and 3, we observe that the off-the-shelf approach fails to accurately predict a grasp on the referred object. This occurs because the query contains attributes like “rightmost” and “furthest” increasing the complexity of referring. Since the masks are

¹GraspAnything++ is open-sourced; however, its public subset is much smaller than the full training data, making fair benchmarking impossible.

Model	Epochs to Conv.	OCID-VLG	RefGraspNet	
			Test Seen	Test Unseen
DetSeg + CLIP [1]	22	28.12 / 39.21	40.19 / 41.56	27.18 / 27.20
GR-ConvNet + CLIP [20]	15	9.73 / 15.41	34.19 / 46.56	30.19 / 32.17
SSG + CLIP [52]	41	33.51 / 34.70	48.78 / 50.10	14.36 / 14.89
Molmo+SAM2+GraspNet	—	63.22 / 69.14	68.85 / 70.27	66.23 / 69.41
CROG [44]	50	77.22 / 87.71	85.32 / 86.49	70.81 / 71.99
HiFi-CS [2]	44	70.54 / 79.12	73.27 / 74.55	62.13 / 63.28
ETRG [55]	49	82.28 / 91.12	86.13/88.12	68.11 / 70.05
Ours: MapleGrasp	32	88.15 / 92.98	89.86 / 91.67	76.92 / 77.67

Table 2. Benchmarking MapleGrasp across OCID-VLG and RefGraspNet datasets for 4-DoF and 6-DoF vision-language driven grasping respectively. Scores reported as grasping accuracy for top-1/top-5 predictions (see Sec. 3.5).













Referring Text	Molmo+SAM+GraspNet	CROG	MapleGrasp
Grasp the rightmost red food box			
Grab the transparent food bag			
Find the banana furthest away from me			
Pass the tissues to the rear left of the blue and black marker			

Table 3. Qualitative comparisons of LDRG approaches under complex referring queries. The zero-shot baseline (first column) struggles to identify referred object due to distractors. MapleGrasp (last column) can predict an accurate and accessible grasp for queried objects in the first three rows. Last row shows an example where all models fail to recognize the correct object (ground truth in green).

predicted incorrectly, the downstream GraspNet predicts an incorrect grasp. While CROG recognizes these objects better, having seen a variety of referring attributes during train-

ing, often fails to localize the grasp within the target object. MapleGrasp’s mask-guided predictions are accurate in first three rows, but fail for occluded objects and ambigu-

ous queries, where the mask alone cannot localize the grasp pose (row 4). More examples in supplementary Sec. S2.

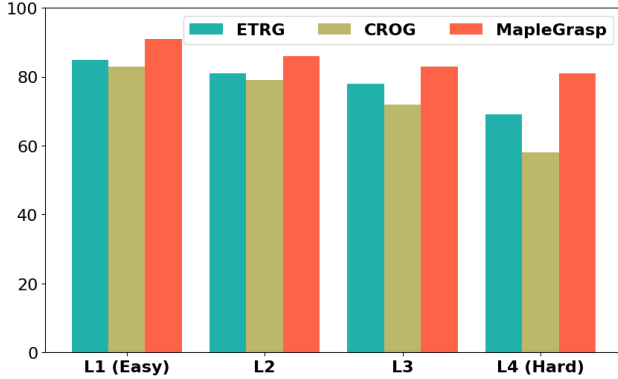


Figure 5. Comparisons across text inputs: from level 1 with just object names to level 4 with color, shape, position attributes

To compare methods across language complexity, we group test queries by the number of object attributes they mention. For example, “Grasp the red circular box near the top right of the image” contains three attributes that an LDRG model must exploit to locate a grasp. Using a popular named entity recognition model, GLiNER [57], we count attributes in the RefGraspNet test split and assign queries to four bands—L1 EASY (one attribute) through L4 HARD (four). Fig. 5 plots Top-1 accuracy for MapleGrasp and two baselines: accuracy declines with added attributes, yet MapleGrasp consistently remains ahead.

We conduct ablation studies on MapleGrasp (Tab. 4) to analyze its effects due to architectural modifications. Results highlight the importance of accurate RES for mask pooling; using Molmo, which achieves lower IoU (50-60%) on object mask detection, negatively impacts grasp accuracy due to complex referring queries requiring task-specific visual grounding. While using frozen CLIP improves object identification, it reduces grasp scores due to insufficient grounding of VL features for grasp detection. Replacing cross-attention with MLP-Mixers [42], does not improve performance. Furthermore, replacing the weighted smooth L1 loss with a standard smooth L1 loss leads to reduced scores due to slower convergence. All ablations use a fixed number of training epochs.

Method	Top-1	Top-5
MapleGrasp	88.15	92.90
(1) Molmo+SAM for Mask Pooling	78.69	81.27
(2) Frozen CLIP Layers	73.14	75.57
(3) No Cross-Attn, MLP-Mixer	85.42	91.54
(4) Standard Smooth L1 Loss	84.35	90.23

Table 4. Ablation study on the OCID-VLG corpus.

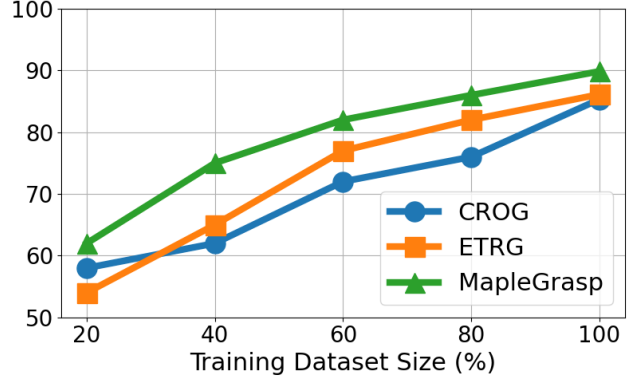


Figure 6. Training data efficiency comparisons across baselines on RefGraspNet. Scores reported as grasping success rate in %.

Model	Train-Dataset	OCID-VLG		RefGraspNet	
		Top-1	Top-5	Top-1	Top-5
CROG	OCID-VLG	77.2	87.7	41.8	42.9
	RefGraspNet	68.2	73.8	85.32	86.49
MapleGrasp	OCID-VLG	88.2	92.9	43.2	45.6
	RefGraspNet	79.5	81.7	89.2	89.7

Table 5. Cross-dataset evaluation results (highlighted). Models trained on RefGraspNet generalize better than OCID-VLG.

Lastly, we evaluate the training efficiency of MapleGrasp in comparison to two baseline methods. In this experiment, we vary the size of the training dataset and assess model performance after training on 20%, 40%, 60%, 80%, and 100% of the RefGraspNet corpus. The results, presented in Fig. 6, demonstrate that MapleGrasp consistently outperforms the baselines on the test set as the dataset size increases, with particularly notable improvements observed after training on just 20–40% of the data. These findings suggest that incorporating referring object masks for pooling vision-language feature maps in grasp detection enhances both training effectiveness and sample efficiency.

5.3. Cross-Dataset Testing

To assess generalizability of models trained on RefGraspNet, we cross-test them on the OCID-VLG benchmark. We compare CROG and MapleGrasp Tab. 5 and our findings reveal that models trained on RefGraspNet generalize better than those trained solely on OCID-VLG.

5.4. LIBERO Physics Simulation Experiments

We test MapleGrasp in the LIBERO simulation environment in a table-top setting. The grasp poses generated by MapleGrasp are executed with an inverse kinematics velocity controller described in supplementary Sec. S3. We compare our modular grasping+trajectory optimization method with end-to-end VLAs. While VLAs are trained on teleoperated demonstrations of successful tasks, we use these observations to identify stable grasp poses for referred objects. We only benchmark the object grasping skill. For ex-

ample, consider the task “Put the wine bottle on the rack.” We consider the task to be successful if the robot grasps the “wine bottle” and lift it above the ground. Success rate is measured manually and averaged with 10 trial runs per task.

Model	SPATIAL	GOAL	OBJECT
Diffusion Policy	77	69	92
Octo	78	84	88
OpenVLA	84	79	90
MapleGrasp	87	85	90

Table 6. Libero simulation results across SPATIAL, GOAL and OBJECT task suites. Scores are reported using success rate

Experiments are conducted on three task suites from the LIBERO benchmark: SPATIAL, GOAL, and OBJECT. For more details about the tasks, refer to supplementary Sec. S4. Results in Tab. 6 compare our method with VLA and diffusion baselines. Our results demonstrate that our grasping+control pipeline achieves similar accuracy to recent VLAs in grasping tasks. Interestingly, decoupling grasping and control improves generalization, as trajectory-based imitation learning methods fail to complete unseen tasks. However, our model successfully determines grasp poses for similar but unseen objects, allowing the control algorithm to generate a stable trajectory without requiring video demonstrations. Cross-dataset testing in Tab. 7 reveals the capabilities of our approach in handling unseen queries across task suites. Since our LDRG model is only concerned with predicting grasp poses and we leverage a controller to determine the trajectory, our method can be deployed without learning from tele-operated demonstrations.

5.5. Real-Robot Experiments

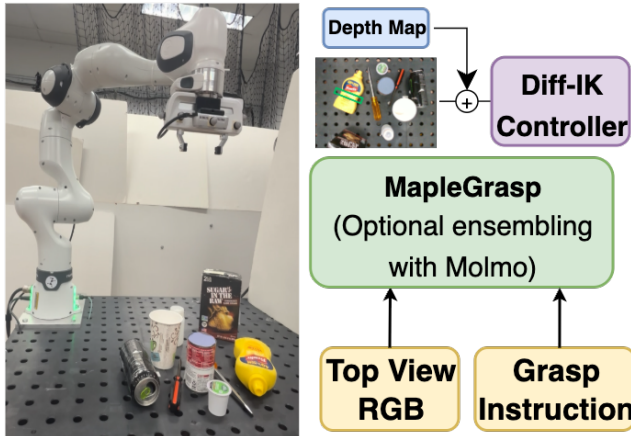


Figure 7. Setup for robot trials using 7 DoF Franka arm.

We evaluate various LDRG methods in a real-world robotic setup using a Franka arm with a camera mounted at the gripper, as shown in Fig. 7. All models were fine-tuned on a combined dataset of RefGraspNet and OCID-VLG. For evaluation, we collected 15 objects, 10 seen and 5 unseen to

Model	Train-Dataset	GOAL	OBJECT
OpenVLA	GOAL	79	0
	OBJECT	12	90
MapleGrasp	GOAL	85	62
	OBJECT	68	90

Table 7. Cross-dataset results show OpenVLA struggles on seen objects in new tasks, while MapleGrasp generalizes better.

create randomly arranged tabletop scenes (see supplementary Sec. S5). To test capabilities of all baselines, we performed separate experiments trying to grasp seen and unseen objects in the presence of distractors (objects that look similar to the target object either in shape, color, or type). Each grasping instruction was tested 10 times and averaged. This resulted in $N = 300$ ($15 \times 2 \times 10$) robot trials. Results are presented in Tab. 8. We consider a trial to be successful if the robot grasps object and lifts it 30cm above the surface.

In the first column (seen objects) all methods tackle the simplest case, having seen these items during training. MapleGrasp leads with a 93% success rate, ahead of CROG and HiFi-CS. The second column adds clutter; varied language queries and distractors lower accuracy for every model, yet MapleGrasp still tops the chart at 87%. The final two rows probe zero-shot grasping of unseen items. Here the Molmo+SAM2+GraspNet baseline rivals MapleGrasp because Molmo—a VLM pre-trained on millions of images spanning thousands of categories—can robustly identify novel targets for GraspNet. To harness this open-world knowledge we form MapleGrasp+Molmo: at inference we compare MapleGrasp’s segmentation mask with Molmo’s out-of-vocabulary prediction, and when MapleGrasp’s confidence is low we keep the mask with the highest overlap before pooling features for the grasp decoder. This strategy lifts success on cluttered scenes with unseen objects to 73%, the best overall. Our two-stage training uses object masks as priors, enabling ensembling with an open-set VLM (see supplementary video for examples).

Model	Seen Objects		Unseen objects	
	Single	Cluttered	Single	Cluttered
Molmo+SAM2+GraspNet	70	61	71	66
HiFi-CS	72	63	65	59
CROG	85	73	69	54
MapleGrasp	93	87	72	65
MapleGrasp+Molmo	91	85	74	73

Table 8. Real robot experiments. Success rate measured across 10 trials for every grasp instruction.

6. Conclusion

Our results highlight mask-guided feature pooling as a simple yet effective technique for language-driven robotic grasping. By selectively pooling predictions within target

regions, MapleGrasp reduces misidentifications and grasp errors in cluttered environments. Our two-stage training strategy, which first predicts segmentation masks and subsequently refines grasp predictions, further enhances accuracy and computational efficiency. Compared to end-to-end vision-language-action models, our modular approach demonstrates superior scalability and robustness, and enables rapid adaptation using readily available vision-language models. Moreover, these systems eliminate the need for time-intensive teleoperated demonstrations and can be customized using a small corpus of RGB-text-grasp annotations. Real-world validation confirms significant improvements in grasp accuracy and efficiency.

References

- [1] Stefan Ainetter and Friedrich Fraundorfer. End-to-end trainable deep neural network for robotic grasp detection and semantic segmentation from rgb. In *2021 IEEE International Conference on Robotics and Automation (ICRA)*, pages 13452–13458, 2021. 2, 6
- [2] Vineet Bhat, Prashanth Krishnamurthy, Ramesh Karri, and Farshad Khorrami. Hifi-cs: Towards open vocabulary visual grounding for robotic grasping using vision-language models, 2024. 2, 5, 6
- [3] Anthony Brohan, Noah Brown, Justice Carbajal, Yevgen Chebotar, Xi Chen, et al. RT-2: Vision-language-action models transfer web knowledge to robotic control. In *arXiv*, 2023. 1
- [4] Open X-Embodiment Collaboration, Abby O’Neill, Abdul Rehman, et al. Open X-Embodiment: Robotic learning datasets and RT-X models. <https://arxiv.org/abs/2310.08864>, 2023. 3
- [5] Aidan Curtis, Nishanth Kumar, Jing Cao, Tomás Lozano-Pérez, and Leslie Pack Kaelbling. Trust the PRoc3s: Solving long-horizon robotics problems with LLMs and constraint satisfaction. In *8th Annual Conference on Robot Learning*, 2024. 2
- [6] Matt Deitke, Christopher Clark, Sangho Lee, Rohun Tripathi, Yue Yang, Jae Sung Park, Mohammadreza Salehi, Niklas Muennighoff, Kyle Lo, Luca Soldaini, Jiasen Lu, Taira Anderson, Erin Bransom, Kiana Ehsani, Huong Ngo, YenSung Chen, Ajay Patel, Mark Yatskar, Chris Callison-Burch, Andrew Head, Rose Hendrix, Favyen Bastani, Eli VanderBilt, Nathan Lambert, Yvonne Chou, Arnavi Chheda, Jenna Sparks, Sam Skjonsberg, Michael Schmitz, Aaron Sarnat, Byron Bischoff, Pete Walsh, Chris Newell, Piper Wolters, Tanmay Gupta, Kuo-Hao Zeng, Jon Borchardt, Dirk Groeneveld, Crystal Nam, Sophie Lebrecht, Caitlin Wittliff, Carissa Schoenick, Oscar Michel, Ranjay Krishna, Luca Weihs, Noah A. Smith, Hannaneh Hajishirzi, Ross Girshick, Ali Farhadi, and Aniruddha Kembhavi. Molmo and pixmo: Open weights and open data for state-of-the-art vision-language models, 2024. 2, 5
- [7] Amaury Depierre, Emmanuel Dellandréa, and Liming Chen. Jacquard: A large scale dataset for robotic grasp detection. In *2018 IEEE/RSJ International Conference on Intelligent Robots and Systems (IROS)*, pages 3511–3516, 2018. 2, 5
- [8] Abhay Deshpande, Yuquan Deng, Arijit Ray, Jordi Salvador, Winson Han, Jiafei Duan, Kuo-Hao Zeng, Yuke Zhu, Ranjay Krishna, and Rose Hendrix. Graspmolmo: Generalizable task-oriented grasping via large-scale synthetic data generation. *arXiv preprint arXiv:2505.13441*, 2025. 2, 4
- [9] Clemens Eppner, Arsalan Mousavian, and Dieter Fox. Acronym: A large-scale grasp dataset based on simulation. In *2021 IEEE International Conference on Robotics and Automation (ICRA)*, pages 6222–6227, 2021. 2, 5
- [10] Hao-Shu Fang, Chenxi Wang, et al. GraspNet-1Billion: A large-scale benchmark for general object grasping. In *Proc. of the IEEE/CVF Conference on Computer Vision and Pattern Recognition*, 2020. 4, 5
- [11] Jensen Gao, Bidipta Sarkar, Fei Xia, Ted Xiao, Jiajun Wu, et al. Physically grounded vision-language models for robotic manipulation. In *IEEE International Conference on Robotics and Automation*, 2024. 1
- [12] Ankit Goyal, Valts Blukis, Jie Xu, Yijie Guo, Yu-Wei Chao, and Dieter Fox. Rvt2: Learning precise manipulation from few demonstrations. *RSS*, 2024. 3
- [13] Daniel Honerkamp, Martin Büchner, Fabien Despinoy, Tim Welschehold, , and Abhinav Valada. Language-grounded dynamic scene graphs for interactive object search with mobile manipulation. *IEEE Robotics and Automation Letters*, 2024. 2
- [14] Wenlong Huang, Fei Xia, Ted Xiao, Harris Chan, Jacky Liang, Pete Florence, Andy Zeng, Jonathan Tompson, Igor Mordatch, Yevgen Chebotar, Pierre Sermanet, Tomas Jackson, Noah Brown, Linda Luu, Sergey Levine, Karol Hausman, and brian ichter. Inner monologue: Embodied reasoning through planning with language models. In *Proceedings of The 6th Conference on Robot Learning*, pages 1769–1782. PMLR, 2023. 2
- [15] Yun Jiang, Stephen Moseson, and Ashutosh Saxena. Efficient grasping from rgb-d images: Learning using a new rect-angle representation. In *2011 IEEE International Conference on Robotics and Automation*, pages 3304–3311, 2011. 2
- [16] Siddharth Karamcheti, Suraj Nair, Ashwin Balakrishna, Percy Liang, Thomas Kollar, and Dorsa Sadigh. Prismatic vlms: Investigating the design space of visually-conditioned language models. In *International Conference on Machine Learning (ICML)*, 2024. 3
- [17] Moo Jin Kim, Karl Pertsch, Siddharth Karamcheti, Ted Xiao, Ashwin Balakrishna, Suraj Nair, Rafael Rafailov, Ethan Foster, Grace Lam, Pannag Sanketi, Quan Vuong, Thomas Kollar, Benjamin Burchfiel, Russ Tedrake, Dorsa Sadigh, Sergey Levine, Percy Liang, and Chelsea Finn. Openvla: An open-source vision-language-action model. *arXiv preprint arXiv:2406.09246*, 2024. 3
- [18] Moo Jin Kim, Chelsea Finn, and Percy Liang. Fine-tuning vision-language-action models: Optimizing speed and success. *arXiv preprint arXiv:2502.19645*, 2025. 2, 3
- [19] Alexander Kirillov, Eric Mintun, Nikhila Ravi, Hanzi Mao, Chloe Rolland, et al. Segment anything. In *Proc. of the IEEE/CVF International Conference on Computer Vision*, 2023. 2

- [20] Sulabh Kumra, Shirin Joshi, and Ferat Sahin. Antipodal robotic grasping using generative residual convolutional neural network. In *2020 IEEE/RSJ International Conference on Intelligent Robots and Systems (IROS)*, pages 9626–9633, 2020. 2, 6
- [21] Meng Li, Qi Zhao, Shuchang Lyu, Chunlei Wang, Yujing Ma, Guangliang Cheng, and Chenguang Yang. Ovgnet: A unified visual-linguistic framework for open-vocabulary robotic grasping. In *2024 IEEE/RSJ International Conference on Intelligent Robots and Systems (IROS)*, pages 7507–7513, 2024. 5
- [22] Meng Li, Qi Zhao, Shuchang Lyu, Chunlei Wang, Yujing Ma, Guangliang Cheng, and Chenguang Yang. Ovgnet: A unified visual-linguistic framework for open-vocabulary robotic grasping. In *2024 IEEE/RSJ International Conference on Intelligent Robots and Systems (IROS)*, pages 7507–7513, 2024. 2
- [23] Xinghang Li, Minghuan Liu, Hanbo Zhang, Cunjun Yu, Jie Xu, Hongtao Wu, Chilam Cheang, Ya Jing, Weinan Zhang, Huaping Liu, Hang Li, and Tao Kong. Vision-language foundation models as effective robot imitators. In *The Twelfth International Conference on Learning Representations*, 2024. 1
- [24] Xiang Li, Cristina Mata, Jongwoo Park, Kumara Kahatapitiya, Yoo Sung Jang, Jinghuan Shang, Kanchana Ranasinghe, Ryan Burgert, Mu Cai, Yong Jae Lee, and Michael S. Ryoo. Llara: Supercharging robot learning data for vision-language policy. In *International Conference on Learning Representations*, 2025. 3
- [25] Peiqi Liu, Yaswanth Orru, Jay Vakil, Chris Paxton, Nur Muhammad Mahi Shafiullah, and Lerrel Pinto. Ok-robot: What really matters in integrating open-knowledge models for robotics. *arXiv preprint arXiv:2401.12202*, 2024. 2
- [26] Shilong Liu, Zhaoyang Zeng, et al. Grounding dino: Marrying dino with grounded pre-training for open-set object detection. *arXiv*, 2023. 2
- [27] Sichao Liu, Jianjing Zhang, Robert X. Gao, Xi Vincent Wang, and Lihui Wang. Vision-language model-driven scene understanding and robotic object manipulation. In *2024 IEEE 20th International Conference on Automation Science and Engineering (CASE)*, pages 21–26, 2024. 1
- [28] Haoyu Lu, Wen Liu, Bo Zhang, Bingxuan Wang, Kai Dong, Bo Liu, Jingxiang Sun, Tongzheng Ren, Zhuoshu Li, Hao Yang, Yaofeng Sun, Chengqi Deng, Hanwei Xu, Zhenda Xie, and Chong Ruan. Deepseek-vl: Towards real-world vision-language understanding, 2024. 3, 4
- [29] Yuhao Lu, Beixing Deng, Zhenyu Wang, Peiyuan Zhi, Yali Li, and Shengjin Wang. Hybrid physical metric for 6-dof grasp pose detection. In *2022 International Conference on Robotics and Automation (ICRA)*, pages 8238–8244, 2022. 2
- [30] Yuhao Lu, Yixuan Fan, Beixing Deng, Fangfu Liu, Yali Li, and Shengjin Wang. Vl-grasp: a 6-dof interactive grasp policy for language-oriented objects in cluttered indoor scenes. In *2023 IEEE/RSJ International Conference on Intelligent Robots and Systems (IROS)*, pages 976–983, 2023. 2, 5
- [31] Huy Hoang Nguyen, An Vuong, Anh Nguyen, Ian Reid, and Minh Nhat Vu. Graspmbamba: A mamba-based language-driven grasp detection framework with hierarchical feature learning. *arXiv preprint arXiv:2409.14403*, 2024. 2, 4
- [32] Nghia Nguyen, Minh Nhat Vu, Baoru Huang, An Vuong, Ngan Le, Thieu Vo, and Anh Nguyen. Lightweight language-driven grasp detection using conditional consistency model. In *2024 IEEE/RSJ International Conference on Intelligent Robots and Systems (IROS)*, pages 13719–13725, 2024. 2
- [33] Toan Nguyen, Minh Nhat Vu, Baoru Huang, An Vuong, Quan Vuong, Ngan Le, Thieu Vo, and Anh Nguyen. Language-driven 6-dof grasp detection using negative prompt guidance. In *Computer Vision – ECCV 2024: 18th European Conference, Milan, Italy, September 29–October 4, 2024, Proceedings, Part XIX*, page 363–381, Berlin, Heidelberg, 2024. Springer-Verlag. 2
- [34] Sangjun Noh, Jongwon Kim, Dongwoo Nam, Seunghyeok Back, Raeyoung Kang, and Kyoobin Lee. GraspSAM: When segment anything model meets grasp detection. *arXiv preprint arXiv:2409.12521*, 2024. 2
- [35] Shengyi Qian, Kaichun Mo, Valts Blukis, David F Fouhey, Dieter Fox, and Ankit Goyal. 3d-mvp: 3d multi-view pretraining for robotic manipulation. *arXiv preprint arXiv:2406.18158*, 2024. 3
- [36] Krishan Rana, Jesse Haviland, Sourav Garg, Jad AbouChakra, Ian Reid, and Niko Suenderhauf. Sayplan: Grounding large language models using 3d scene graphs for scalable task planning. In *7th Annual Conference on Robot Learning*, 2023. 2
- [37] Nikhila Ravi, Valentin Gabeur, Yuan-Ting Hu, Ronghang Hu, Chaitanya Ryali, Tengyu Ma, Haitham Khedr, Roman Rädle, Chloe Rolland, Laura Gustafson, Eric Mintun, Junting Pan, Kalyan Vasudev Alwala, Nicolas Carion, Chao-Yuan Wu, Ross Girshick, Piotr Dollar, and Christoph Feichtenhofer. SAM 2: Segment anything in images and videos. In *The Thirteenth International Conference on Learning Representations*, 2025. 5
- [38] Chan Hee Song, Jiaman Wu, Clayton Washington, Brian M. Sadler, Wei-Lun Chao, and Yu Su. Llm-planner: Few-shot grounded planning for embodied agents with large language models. In *Proceedings of the IEEE/CVF International Conference on Computer Vision (ICCV)*, 2023. 2
- [39] Shuran Song, Andy Zeng, Johnny Lee, and Thomas Funkhouser. Grasping in the wild: Learning 6dof closed-loop grasping from low-cost demonstrations. *IEEE Robotics and Automation Letters*, 5(3):4978–4985, 2020. 2
- [40] Martin Sundermeyer, Arsalan Mousavian, Rudolph Triebel, and Dieter Fox. Contact-graspnet: Efficient 6-dof grasp generation in cluttered scenes. 2021. 3, 4
- [41] Chao Tang, Dehao Huang, Wenlong Dong, Ruinian Xu, and Hong Zhang. Foundationgrasp: Generalizable task-oriented grasping with foundation models. *IEEE Transactions on Automation Science and Engineering*, 22:12418–12435, 2025. 2
- [42] Ilya O Tolstikhin, Neil Houlsby, Alexander Kolesnikov, Lucas Beyer, Xiaohua Zhai, Thomas Unterthiner, Jessica Yung, Andreas Steiner, Daniel Keysers, Jakob Uszkoreit, Mario Lucic, and Alexey Dosovitskiy. Mlp-mixer: An all-mlp architecture for vision. In *Advances in Neural Information*

- Processing Systems*, pages 24261–24272. Curran Associates, Inc., 2021. 7
- [43] Georgios Tzifas and Hamidreza Kasaei. Towards open-world grasping with large vision-language models. In *8th Annual Conference on Robot Learning*, 2024. 2
 - [44] Georgios Tzifas, Yucheng XU, Arushi Goel, Mohammadreza Kasaei, Zhibin Li, and Hamidreza Kasaei. Language-guided robot grasping: Clip-based referring grasp synthesis in clutter. In *Proceedings of The 7th Conference on Robot Learning*, pages 1450–1466. PMLR, 2023. 2, 4, 5, 6
 - [45] Tuan Van Vo, Minh Nhat Vu, Baoru Huang, An Vuong, Ngan Le, Thieu Vo, and Anh Nguyen. Language-driven grasp detection with mask-guided attention. In *2024 IEEE/RSJ International Conference on Intelligent Robots and Systems (IROS)*, pages 7492–7498, 2024. 2, 4
 - [46] A. D. Vuong, M. N. Vu, H. Le, B. Huang, H. T. T. Binh, T. Vo, A. Kugi, and A. Nguyen. Grasp-anything: Large-scale grasp dataset from foundation models. In *2024 IEEE International Conference on Robotics and Automation (ICRA)*, pages 14030–14037, 2024. 2
 - [47] A. D. Vuong, M. N. Vu, H. Le, B. Huang, H. T. T. Binh, T. Vo, A. Kugi, and A. Nguyen. Grasp-anything: Large-scale grasp dataset from foundation models. In *2024 IEEE International Conference on Robotics and Automation (ICRA)*, pages 14030–14037, 2024. 2, 5
 - [48] Naoki Wake, Atsushi Kanehira, Kazuhiro Sasabuchi, Jun Takamatsu, and Katsushi Ikeuchi. Gpt-4v(ision) for robotics: Multimodal task planning from human demonstration. *IEEE Robotics and Automation Letters*, 9(11):10567–10574, 2024. 3
 - [49] Yi-Lin Wei, Jian-Jian Jiang, Chengyi Xing, Xian-Tuo Tan, Xiao-Ming Wu, Hao Li, Mark Cutkosky, and Wei-Shi Zheng. Grasp as you say: Language-guided dexterous grasp generation. In *Advances in Neural Information Processing Systems*, pages 46881–46907. Curran Associates, Inc., 2024. 2
 - [50] Jimmy Wu, Rika Antonova, Adam Kan, Marion Lepert, Andy Zeng, Shuran Song, Jeannette Bohg, Szymon Rusinkiewicz, and Thomas Funkhouser. Tidybot: Personalized robot assistance with large language models. In *2023 IEEE/RSJ International Conference on Intelligent Robots and Systems (IROS)*, pages 3546–3553, 2023. 1
 - [51] Kechun Xu, Shuqi Zhao, Zhongxiang Zhou, Zizhang Li, Huaijin Pi, Yifeng Zhu, Yue Wang, and Rong Xiong. A joint modeling of vision-language-action for target-oriented grasping in clutter. In *2023 IEEE International Conference on Robotics and Automation (ICRA)*, pages 11597–11604, 2023. 1, 2
 - [52] Yucheng Xu, Mohammadreza Kasaei, Hamidreza Kasaei, and Zhibin Li. Instance-wise grasp synthesis for robotic grasping. *arXiv preprint arXiv:2302.07824*, 2023. 6
 - [53] Bin Yan, Yi Jiang, Jiannan Wu, Dong Wang, Zehuan Yuan, Ping Luo, and Huchuan Lu. Universal instance perception as object discovery and retrieval. In *CVPR*, 2023. 2
 - [54] Yuxiang Yang, Jiangtao Guo, Zilong Li, Zhiwei He, and Jing Zhang. Ground4act: Leveraging visual-language model for collaborative pushing and grasping in clutter. *Image and Vision Computing*, 151:105280, 2024. 2
 - [55] Houjian Yu, Mingen Li, Alireza Rezazadeh, Yang Yang, and Changhyun Choi. A parameter-efficient tuning framework for language-guided object grounding and robot grasping. *arXiv preprint arXiv:2409.19457*, 2024. 2, 5, 6
 - [56] Sheng Yu, Di-Hua Zhai, Yuanqing Xia, Haoran Wu, and Jun Liao. Se-resunet: A novel robotic grasp detection method. *IEEE Robotics and Automation Letters*, 7(2):5238–5245, 2022. 2
 - [57] Urchade Zaratiana, Nadi Tomeh, Pierre Holat, and Thierry Charnois. GLiNER: Generalist model for named entity recognition using bidirectional transformer. In *Proceedings of the 2024 Conference of the North American Chapter of the Association for Computational Linguistics: Human Language Technologies (Volume 1: Long Papers)*, pages 5364–5376, Mexico City, Mexico, 2024. Association for Computational Linguistics. 7
 - [58] Xiaohua Zhai, Basil Mustafa, Alexander Kolesnikov, and Lucas Beyer. Sigmoid loss for language image pre-training. In *Proceedings of the IEEE/CVF International Conference on Computer Vision (ICCV)*, pages 11975–11986, 2023. 3
 - [59] Hanbo Zhang, Xuguang Lan, Site Bai, Xinwen Zhou, Zhiqiang Tian, and Nanning Zheng. Roi-based robotic grasp detection for object overlapping scenes. In *2019 IEEE/RSJ International Conference on Intelligent Robots and Systems (IROS)*, pages 4768–4775, 2019. 5
 - [60] Yuxuan Zhang, Tianheng Cheng, Rui Hu, Lei Liu, Heng Liu, Longjin Ran, Xiaoxin Chen, Wenyu Liu, and Xinggang Wang. Evf-sam: Early vision-language fusion for text-prompted segment anything model. *arXiv preprint arXiv:2406.20076*, 2024. 2
 - [61] Min Zhao, Guoyu Zuo, Shuangyue Yu, Yongkang Luo, Chunfang Liu, and Daoxiong Gong. Language-guided category push-grasp synergy learning in clutter by efficiently perceiving object manipulation space. *IEEE Transactions on Industrial Informatics*, 21(2):1783–1792, 2025. 2
 - [62] Wentao Zhao, Jiaming Chen, Ziyu Meng, Donghui Mao, Ran Song, and Wei Zhang. Vlmcp: Vision-language model predictive control for robotic manipulation. In *Robotics: Science and Systems*, 2024. 1
 - [63] Haiyue Zhu, Yiting Li, Fengjun Bai, Wenjie Chen, Xiaocong Li, Jun Ma, Chek Sing Teo, Pey Yuen Tao, and Wei Lin. Grasping detection network with uncertainty estimation for confidence-driven semi-supervised domain adaptation. In *2020 IEEE/RSJ International Conference on Intelligent Robots and Systems (IROS)*, pages 9608–9613, 2020. 2